FLUIDIC SELF-ASSEMBLY OF MILLIMETER SCALE THIN PARTS ON PREPROGRAMMED SUBSTRATE AT AIR-WATER INTERFACE

Kwang Soon Park[1], Xugang Xiong[1], Rajashree Baskaran[2], Karl F Böhringer[1]
[1]Department of Electrical Engineering, University of Washington, Seattle, USA
[2]Components Research, Intel Corporation, USA

Abstract

This paper presents a novel method to achieve high yield assembly of millimeter-scale thin silicon chips from an air-water interface. Surface functionalized silicon parts (1000×1000×100 μm^3) assemble in preprogrammed hydrophilic locations on a wafer substrate with self-alignment. We optimized the process and design factors systematically using DOE (Design of Experiment) that leads to high yield (100 %).

1. Introduction

Fluidic self-assembly (FSA) is a promising alternative to conventional serial pick-and-place assembly. The serial pick-and-place mechanical assembly enables high yield. For small size parts, however, it becomes slow and difficult to control due to undesirable strong stiction forces. Therefore, for assembly of large numbers of small and thin parts, conventional pick-and-place becomes costly and FSA is preferred. Previous FSA systems have used various driving forces such as gravity, surface tension, electrostatic or electromagnetic force and often require adhesives, liquid solder, shape matching structures or two different liquids [1]. They, however, have lower yield compared to pick-and-place assembly due to their stochastic nature [2]. In this paper, we demonstrate a high-yield FSA using specific surface Faraday waves to perform selective assembly from excess part supply to programmed sites.

2. FSA system setup

Our system consists of a water container on a linear electromagnetic vertical vibration table and a dip coater, substrate and parts floating at an air-water interface (Figure 1). The measured acceleration uniformity over the vibration table is 0.72 % or +/- 10 mg. This is measured using a laser vibrometer (Polytec OFV-534 laser unit and OFV-2500 vibrometer controller) when driven at 80 Hz / 1.4 g. The substrate is tilted at 10° angle with the water surface and vertically pulled up at a constant speed. This angle is optimized from tests which show lower capillary force at higher angle and poor controllability of water/substrate interface position at lower angles when pulled up. During pull-up, parts approach the substrate due to water curvature formed by the hydrophobic (SAM-coated Au) / hydrophilic (Si) patterns on the substrate and become assembled (Figure 2).

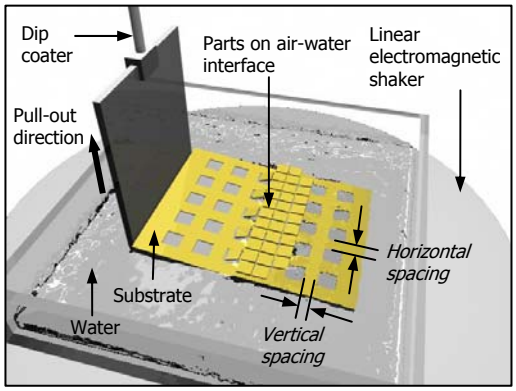

Figure 1. The experimental setup consists of a water container, linear electromagnetic vibration table, dip coater, substrate and parts floating at air-water interface.

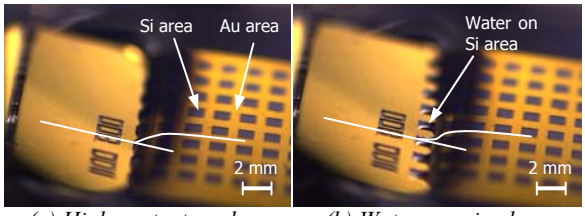

(a) High contact angle for part approaching *(b) Water remained on Si area for part assembly*

Figure 2. Contact angle change at water/substrate during pull-up.

3. Fabrication

The assembly template is fabricated from a 4 inch silicon wafer coated with Cr (10 nm) and Au (100 nm) by electron beam evaporation. The wafer is spin coated with AZ4620 resist followed by photolithography to define the square patterns. The exposed Au and Cr layers are removed subsequently using wet etching. A standard Bosch DRIE (Deep Reactive Ion Etch) process is used to etch the exposed silicon sites to ~70 µm depth. After photoresist removal, the patterned substrate is cleaned in oxygen plasma and then soaked in a solution of 1 mM dodecanethiol in ethanol overnight. A self-assembled monolayer (SAM) of thiol molecules selectively

attaches to the gold surface and makes them hydrophobic [3]. The wafer substrate is then diced into several pieces for assembly tests. Fabrication of 1 mm sized parts is achieved by standard photolithography, Cr/Au evaporation and lift-off steps on the front side of the wafer. After lift-off, a grinding process from the back side of the wafer thins the silicon wafer down to 100 μm, and then the wafer is diced into individual parts and stored in ethanol solution.

4. Parameter selection through screening test

To investigate the factors that influence assembly, nine substrates with different spatial patterns (Table 1) were tested at various frequencies (35/45/55 Hz) and actuator output (1.5/1.75/2.0 g). In this preliminary experiment, the angle between the substrate and water surface is 10° and pull-up speed is 1mm/min. In this range, only Substrate#1 with wider spacing between hydrophilic sites has selective assembly and the highest yield (45 %) at 55 Hz / 1.5 g. The other substrates do not show any selective assembly because narrow spacing does not produce distinct stick-slip motion. From this result, horizontal/vertical spacing, and agitation condition are set as important factors in our experiment.

Table 1. Design factors for screening test.

Substrate	Si area	Horizontal spacing	Vertical spacing
#1	1.2×1.2 mm^2	1.1 mm	1.8 mm
#2		0.8 mm	0.2 mm
#3		0.2 mm	0.8 mm

5. Optimization and verification

Step 1. To analyze the effect of these factors, we use the levels in Table 2 and select full factorial design in fully randomized order to minimize unexpected bias. Based on the previous experiment, horizontal / vertical spacing is determined to be larger than 200 μm to achieve selective assembly. However, a design with 500 μm spacing exhibits no selective assembly and all designs with 35 Hz agitation achieve no assembly. Therefore, 500 μm and 35 Hz are not presented in the analysis.

To measure the contribution of each factor to yield, these experimental data are analyzed. In the effect analysis result in Figure 3, the x-axis for each graph presents the factor levels and the y-axis indicates yield. The higher the slope, the larger is the effect on yield. Horizontal spacing has a larger effect than that of vertical spacing. High frequency (55 Hz) and low acceleration (1.5 g) leads to optimum agitation condition. The results (Table 3, Figure 3~4) show that the yield can be effectively improved by widening horizontal spacing rather than vertical spacing. The contour plots for each substrate in Figure 4 show the same trend that higher frequency and lower acceleration will produce higher yield. Further experimental conditions for optimization, frequency and acceleration range are determined based on contour plots.

Table 2. Design factors with levels. Nine substrate and nine agitation conditions make a total of 81 runs.

Factor	Level
Horizontal spacing	500 / 800 / 1100 μm
Vertical spacing	500 / 800 / 1100 μm
Frequency	35 / 45 / 55 Hz
Acceleration	1.50 / 1.75/ 2.00 g

Table 3. Range and effect of four factors to assembly yield.

Factor	Range	Effective yield change
Horizontal spacing	800/1100 μm	10.4 %
Vertical spacing	800/1100 μm	4.6 %
Frequency	45 / 55 Hz	16.4 %
Acceleration	1.50/1.75/2.00 g	11.3 %

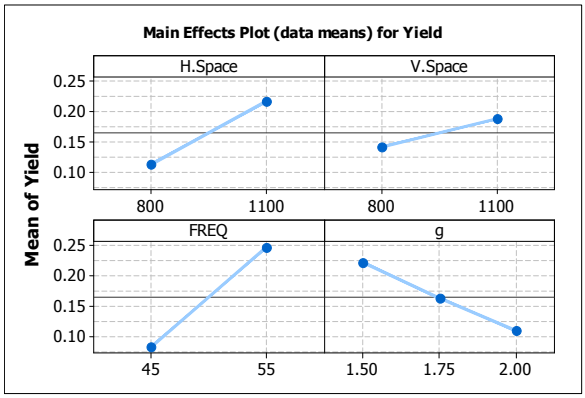

Figure 3. Effect with slope of four factors to assembly yield. X-axis presents the factor levels and Y-axis indicates yield.

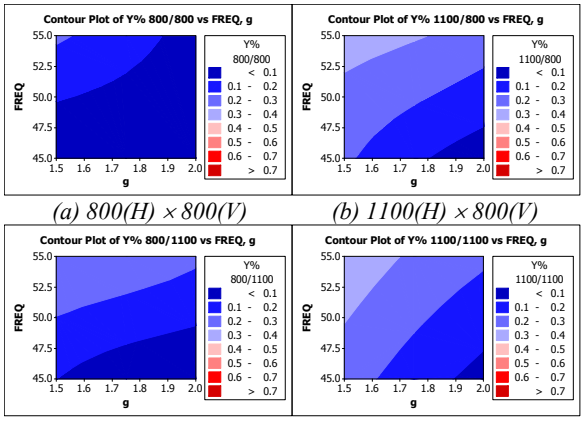

(a) 800(H) × 800(V) *(b) 1100(H) × 800(V)*

(c) 800(H) × 1100(V) *(d) 1100(H) × 1100(V)*

Figure 4. Contour plots of assembly yield versus agitation frequency (x-axis) and amplitude (y-axis) for four substrate designs in Table 3.

Step 2. From the analysis result in Figure 3~4, the optimum agitation condition seems to be in the left upper region of the contour plots. Therefore, to find the optimal agitation condition, full factorial design with four parameters in Table 4 is used. As in Table 4, the same substrates as in step 1 are tested with higher frequencies and wider acceleration values. Full factorial design in fully randomized order is pursued in this step.

Table 4. Design factors with levels. Four substrate and nine agitation conditions make a total of 36 runs.

Factor	Level
Horizontal spacing	800 / 1100 μm
Vertical spacing	800 / 1100 μm
Frequency	65 / 80 / 95 Hz
Acceleration	1.0 / 1.5 / 2.0 g

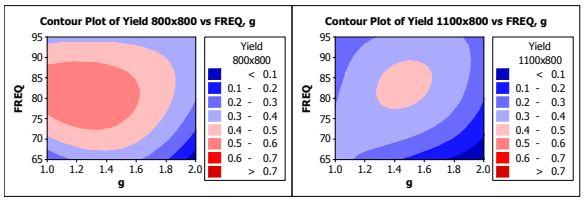

(a) 800(H) × 800(V) *(b) 1100(H) × 800(V)*

(c) 800(H) × 1100(V) *(d) 1100(H) × 1100(V)*

Figure 5. Contour plots of assembly yield versus agitation frequency (x-axis) and amplitude (y-axis) for four substrate designs in Table 4.

Through this additional test, the optimum agitation conditions for four substrates are found to be 80 Hz / 1.4 g. As presented in Figure 5, the optimum agitation conditions can be easily chosen from the contour plots and are almost independent of the horizontal / vertical spacing.

Step 3. To verify the reliability of the experimental data, a method called ANOVA (analysis of variance) is used. In an ANOVA test, total observed variance (SS_T) is partitioned into two components: the treatment sum of squares (SS_{TR}) and the error sum of square (SS_E) depending on the explainability. This relationship can be written as

$$SS_T = SS_{TR} + SS_E \qquad (1)$$

According to the ANOVA result in Table 5, SS_{TR} which is explainable forms 82.8% of total observed variation (SS_T) and is due to the variation of the parameters. The portion of error (SS_E) which is unexplainable is only 17.2 % of the total variation. This error can be caused by uncontrollable factors in the experiment such as repetition, measurement, shaker frequency / amplitude variation and different part distribution on the air-water interface. This analysis assures the reliability of the experiment. In addition, the formula for the one-way ANOVA F-test statistic is

$$F = \frac{MS_{TR}}{MS_E} \qquad (2)$$

Here, the mean squares (MS_{TR} *and* MS_E) are quantities computed by dividing the sum of squares by its number of degrees of freedom [6]. This equation indicates the ratio of explainable variance and unexplainable variance. By comparing the components of the total variation, the statistical significance of treatment is tested. The critical F value is the number that the test statistic must exceed to reject the test and it is determined by the significance level, the number of groups to compare and the degrees of freedom. In our experiment, the critical F value is 4.17 at $\alpha = 0.05$. Since $F = 11.77 > 4.17$, the effect of parameters is proved to be significant at 5 % significance level.

Table 5. Result of analysis of variance.

Source of Variation	Sum of Squares	Degrees of Freedom	Mean Squares	F
Parameters	2.06138	31	0.06650	11.77
Error	0.42936	76	0.00565	
Total	2.49074	107		

6. Effect of Faraday waves and high yield assembly

Typical yield loss in FSA is due to lack of control of one-on-one part to site registration. In our method, the parts are restricted to a surface layer and hence many are available for assembly. We avoid multiple parts approaching a site by use of surface waves. Based on the experimental data, we hypothesize that the actuator temporal frequency dependent Faraday wave spatial frequency is a critical factor that affects selective assembly. This addition of surface Faraday waves is a critical new component in our assembly process design compared with previous FSAs.

To investigate the effect of Faraday waves on parts rearrangement, frequencies from 50 to 100 Hz are applied to form Faraday waves. For a frequency range from 50 to 100 Hz, the wave numbers k are calculated using the equations in [4,5] and compared to theoretical values in Figure 7. At the optimal frequency of this FSA system, the wave length of surface Faraday wave is 6.9 mm. This wave number can be shifted if a substrate and parts are considered. Further study is needed with different boundary conditions.

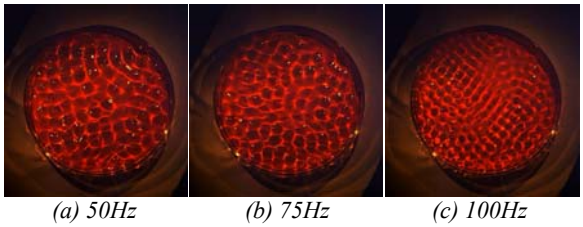

(a) 50Hz (b) 75Hz (c) 100Hz

Figure 6. Faraday wave vs. applied frequency. As frequency increases shorter wavelength (higher k) is observed.

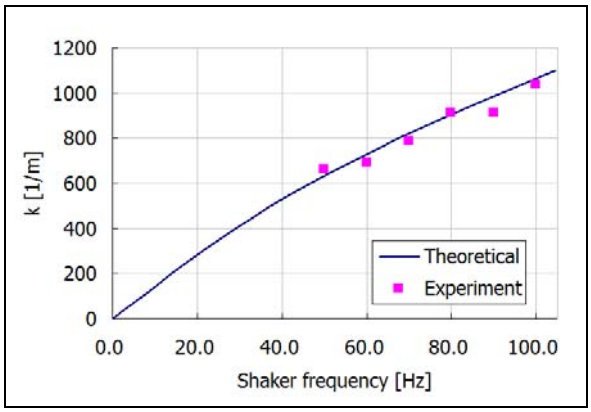

Figure 7. Comparison of k values. Theoretical and experimental values are compared.

This FSA system has highest yield when parts are rearranged by agitation so that only one part faces one binding site as shown in Figure 8(c). The statistical analysis of minimum agitation time for this rearrangement indicates that longer agitation produces higher probability of rearrangement and 50 sec agitation has 99.9988 % probability (= 116.5 ppm error). Based on this, 100 % yield (Figure 6(d)) can be achieved by repeating the following three steps for each row: (i) pull-up without agitation and pause and (ii) agitation (~80 Hz / 1.4 g) for 50 sec and (iii) pull-up for assembly.

Therefore, a high yield FSA system can be constructed using an open-loop system with sufficient agitation time or a closed-loop system for faster process by adding feedback to check parts rearrangement as shown in Figure 8(c).

7. Conclusion

A novel fluidic self-assembly using air-water interface is developed. Four parameters (horizontal and vertical spacing, frequency, acceleration) are selected by screening test and optimized through design of experiment (DOE) method with effect analysis. Surface Faraday waves are introduced to achieve more selective assembly by part rearrangement. In addition, 100% assembly is demonstrated by applying Faraday waves.

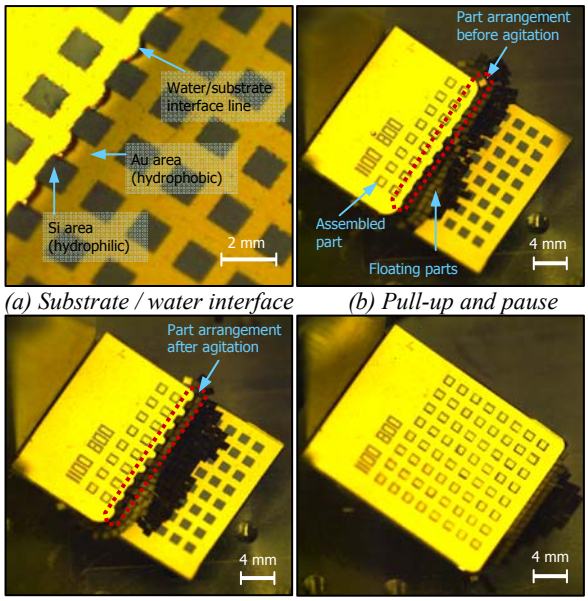

(a) Substrate / water interface (b) Pull-up and pause

(c) After agitation (d) Example of 100% assembly

Figure 8. Parts rearrangement by agitation. Dark squares are hydrophilic sites and gold regions are hydrophobic surfaces.

Acknowledgement

This work was funded by the Center on Interfacial Engineering for Microelectromechanical Systems (CIEMS) under DARPA grant HR0011-06-0049 (Dr. D. L. Polla, Program Manager) and by Intel Corporation.

References

[1] R. Knuesel, S. Bose, W. Zheng and H. O. Jacobs, “Engineered Solder-Directed Self-Assembly Across Length Scales”, Mater. Res. Soc. Symp. Proc., Vol. 990, pp. 313-318, 2007.

[2] M. Boncheva, D. A. Bruzewicz and G. M. Whitesides, “Millimeter-scale self-assembly and its Applications”, Pure Appl. Chem., Vol. 75, No. 5, pp. 621–630, 2003.

[3] X. Xiong, Y. Hanein, J. Fang, Y. Wang, W. Wang, D.T. Schwartz and K.F. Böhringer, “Controlled Multibatch Self-Assembly of Microdevices”, J. Microelectromech. Syst., Vol.12, No.2, pp. 117-127, 2003.

[4] S. Douady and S. Fauve, "Pattern Selection in Faraday Instability", Europhys. Lett., Vol. 6, No. 3, pp. 221-226, 1988.

[5] T. B. Benjamin and F. Ursell, "The Stability of the Plane Free Surface of a Liquid in Vertical Periodic Motion", Proc. R. Soc. Lond. A., Vol.225, No. 1163, pp. 505-515, 1954.

[6] D. C. Montgomery and G. C. Runger, Applied Statistics and Probability for Engineers. New York: Wiley, 2007.